

# Magneto-optical rotation of nonmonochromatic fields and its nonlinear dependence on optical density

G. S. Agarwal and Shubhrangshu Dasgupta

*Physical Research Laboratory, Navrangpura, Ahmedabad-380 009, India*

(Received 11 February 2003; published 11 June 2003)

We calculate magneto-optical rotation of nonmonochromatic fields in an optically thick cold atomic medium. We show that the nonmonochromatic nature leads to a nonlinear dependence of the rotation angle on optical density. Using our calculations, we provide a quantitative analysis of the recent experimental results of Labeyrie *et al.* [Phys. Rev. A **64**, 033402 (2001)] using cold  $^{85}\text{Rb}$  atoms.

DOI: 10.1103/PhysRevA.67.063802

PACS number(s): 42.50.Ct, 33.55.Ad, 32.80.Pj

## I. INTRODUCTION

A very useful way to get important spectroscopic information is by measuring the magneto-optical rotation (MOR) of a plane polarized light propagating through a medium [1]. Clearly, it is desirable to obtain as large an angle of rotation as possible [2,3]. It is known that the angle of rotation is proportional to the density of the medium. Thus an increase in density will help in achieving large rotation angles. Recently, very large rotation angles in a cold sample have been reported [4]. In this experiment, optical densities of the order of 10–20 were achieved. This experiment also reported a very interesting result, viz., a departure from the linear dependence of the rotation angle on the optical density. This departure has been ascribed to the nonmonochromatic nature of the input laser. The findings of the experiment warrant a quantitative analysis of the dependence of the rotation angle on the spectral profile of the input laser. We present a first principles calculation of this dependence. Note that a nonlinear dependence on optical density cannot result from a simple argument based on the standard formula for the rotation angle  $\theta$ :

$$\theta = \pi k l \text{Re}(\chi_- - \chi_+), \quad (1)$$

where  $k$  is the wave number of the electric field,  $l$  is the length of the medium, and  $\chi_{\pm}$  represent the linear susceptibilities of the medium for right or left circularly polarized components of the input field. Since  $\chi_{\pm}$  are proportional to the number density, the rotation angle becomes proportional to the optical density  $\alpha$  defined by

$$\alpha = \frac{3\lambda^2}{2\pi} N l, \quad (2)$$

where  $\lambda = 2\pi/k$  is the wavelength of the input field and  $N$  is the number density of the atomic medium. If one were to argue that a nonmonochromatic laser field would replace  $\chi_{\pm}$  by their averages over the width of the laser, then  $\theta$  would continue to be proportional to the optical density  $\alpha$ . A more quantitative analysis of the rotation angle is thus warranted.

The organization of the paper is as follows. In Sec. II, we recapitulate the relevant equations for studies of MOR in an atomic medium. In Sec. III, we describe a simple three-level atomic configuration in the context of MOR and discuss the

effects of laser line shape and magnetic field in a thick atomic medium. In Sec. IV, we consider the experimental configuration used in [4]. We show how, in an optically thick medium, one deviates from the linear dependence of rotation on optical density as a result of the nonmonochromatic nature of the laser field. We give a quantitative analysis of the experimental data.

## II. BASIC EQUATIONS

Let us consider that an atomic medium of length  $l$  is resonantly excited by a monochromatic  $\hat{x}$ -polarized electric field

$$\vec{E}(z, t) = \hat{x} \mathcal{E} e^{ikz - i\omega t} + \text{c.c.}, \quad (3)$$

where  $\mathcal{E}$  is the field amplitude and  $k = \omega/c = 2\pi/\lambda$  is the wave number of the field,  $\omega$  and  $\lambda$  being the corresponding angular frequency and wavelength. The field is propagating in the  $z$  direction. Clearly, we can resolve the amplitude of the electric field into its two circular components as

$$\hat{x} \mathcal{E} \equiv \hat{e}_+ \mathcal{E}_+ + \hat{e}_- \mathcal{E}_-, \quad (4)$$

where  $\mathcal{E}_{\pm} = \mathcal{E}/\sqrt{2}$  are the amplitude components along two circular polarizations  $\hat{e}_{\pm} = (\hat{x} \pm i\hat{y})/\sqrt{2}$ .

While passing through the atomic medium these two circular components behave differently due to the anisotropy of the medium. Let  $\chi_{\pm}$  be the susceptibilities of the medium corresponding to the two circular components. The electric field at the exit face of the medium can be written as

$$\begin{aligned} \vec{E}(l, t) &= \vec{\mathcal{E}}_l e^{ikz - i\omega t} + \text{c.c.}, \\ \vec{\mathcal{E}}_l &= [\hat{e}_+ \mathcal{E}_+ e^{2\pi i k l \chi_+} + \hat{e}_- \mathcal{E}_- e^{2\pi i k l \chi_-}], \end{aligned} \quad (5)$$

where we have assumed that the medium is dilute so that  $|4\pi\chi_{\pm}| \ll 1$ . In MOR, the polarization direction of the input electric field is rotated due to the difference in their dispersions (phase shifts) in a nonattenuating medium. The electric field, however, remains linearly polarized after passing through the medium. In the present case, because the atom interacts with a near-resonant electric field, the two circular components suffer attenuation (given by the imaginary part of  $\chi_{\pm}$ ) while propagating through the medium. Thus the medium concerned here is responsible for both dispersion and

attenuation. We say that the medium is both circularly birefringent and circularly dichroic. The output electric field becomes elliptically polarized under the action of such a medium. Thus, to fully characterize the polarization state of the output field, one has to use the Stokes parameters [5]. The four Stokes parameters for an electric field are designated by  $S_\alpha$  ( $\alpha=0,1,2,3$ ) and can be defined as follows:

$$S_0 = I_{\parallel} + I_{\perp}, \quad (6a)$$

$$S_1 = I_{\parallel} - I_{\perp}, \quad (6b)$$

$$S_2 = I_{45^\circ} - I_{-45^\circ}, \quad (6c)$$

$$S_3 = I_{\sigma_+} - I_{\sigma_-}, \quad (6d)$$

where  $I_{\hat{n}}$  is the measured intensity along the polarization direction  $\hat{n}$ . Then the output polarization state can be characterized by the following three quantities:

$$P = \frac{\sqrt{S_1^2 + S_2^2 + S_3^2}}{S_0}, \quad (7a)$$

$$\tan 2\theta = \frac{S_2}{S_1} \quad (0 \leq \theta < \pi), \quad (7b)$$

$$\tan 2\phi = \frac{S_3}{S_0 P} \quad (-\pi/4 < \phi \leq \pi/4), \quad (7c)$$

where  $P$  is the degree of polarization, i.e., the ratio of the intensities of the polarized component to those of the unpolarized one,  $\theta$  is the Faraday rotation angle of the input field and is measured between the major axis of the ellipse and the  $x$  axis, and  $\phi$  provides the ellipticity of polarization through the relation  $e = \tan \phi$ .

From Eq. (5) one can express the output intensities along different polarization directions in the following way:

$$I_{\parallel}(\omega) = |\hat{x} \cdot \vec{\mathcal{E}}_l|^2 = \frac{I_0}{4} |e^{2\pi i k l \chi_+} + e^{2\pi i k l \chi_-}|^2, \quad (8a)$$

$$I_{\perp}(\omega) = |\hat{y} \cdot \vec{\mathcal{E}}_l|^2 = \frac{I_0}{4} |e^{2\pi i k l \chi_+} - e^{2\pi i k l \chi_-}|^2, \quad (8b)$$

$$I_{\pm 45^\circ}(\omega) = \left| \frac{\hat{x} \pm \hat{y}}{\sqrt{2}} \cdot \vec{\mathcal{E}}_l \right|^2 = \frac{I_0}{8} |(1 \pm i)e^{2\pi i k l \chi_+} + (1 \mp i)e^{2\pi i k l \chi_-}|^2, \quad (8c)$$

$$I_{\sigma_{\pm}}(\omega) = |\hat{e}_{\pm} \cdot \vec{\mathcal{E}}_l|^2 = \frac{I_0}{2} \exp[-4\pi k l \text{Im}(\chi_{\pm})], \quad (8d)$$

where  $I_0 = |\mathcal{E}|^2$  is the input intensity of laser field.

Note that all the measured quantities defined by Eq. (8) are functions of the frequency of the exciting field. If the exciting field is nonmonochromatic, then the Stokes param-

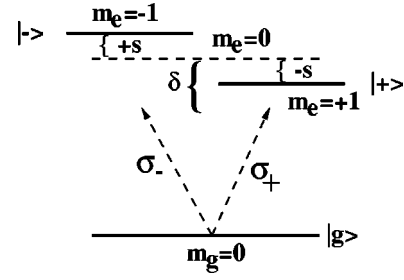


FIG. 1. Level diagram for a three-level configuration. The excited levels  $|\pm\rangle$  ( $m_e = \pm 1$ ) are Zeeman shifted from the level  $m_e = 0$  by an amount  $s$ . The detuning  $\delta$  is defined between the levels  $m_e = 0$  and  $m_g = 0$ .

eters  $\langle S_\alpha \rangle$  are to be obtained by averaging over the spectrum  $S(\omega)$  of the laser field. Thus, the  $I$ 's in Eq. (6) are to be obtained from

$$\langle I_{\hat{n}} \rangle = \frac{1}{I_0} \int_{-\infty}^{\infty} d\omega I_{\hat{n}}(\omega) S(\omega). \quad (9)$$

For simplicity, we can adopt, say, a Lorentzian line shape for the input,

$$S(\omega) \equiv I_0 \frac{\gamma_c / \pi}{\gamma_c^2 + (\omega - \omega_l)^2}, \quad (10)$$

where  $\omega_l$  is the central frequency of the laser field and  $2\gamma_c$  is the full width at half maximum. We will demonstrate how the fluctuations of the input field lead to the nonlinear dependence of the rotation angle on optical density.

### III. A SIMPLIFIED ATOMIC MODEL

We first consider a three-level atom in V configuration (see Fig. 1) in order to uncover the effect of optical density on MOR. The levels  $|\pm\rangle$  ( $J_e = 1, m_e = \pm 1$ ) are coupled to the ground state  $|g\rangle$  ( $J_g = 0, m_g = 0$ ) by two circular components  $\sigma_{\pm}$  of the  $\hat{x}$  polarized electric field [Eq. (3)]. The excited level degeneracy has been removed by a uniform magnetic field  $\vec{B}$  applied in the direction of propagation of the applied electric field. The levels  $|e_{\pm}\rangle$  are shifted about the line center by an amount  $\mp \mu_B B / \hbar$  ( $\mu_B$  is the Bohr magneton). The field  $\vec{E}$  is detuned from the line center by an amount  $\delta = \omega_{+g}(B=0) - \omega$ ,  $\omega_{+g}(B=0)$  being the atomic transition frequency in the absence of the magnetic field.

The susceptibilities of the  $\sigma_{\pm}$  components inside the medium can be written as

$$\chi_{\pm} = \frac{N |\vec{d}|^2}{\hbar \gamma} \rho_{\pm}, \quad \rho_{\pm} = \frac{i \gamma}{\gamma + i(\delta \mp s)}, \quad (11)$$

where  $2\gamma = 4|\vec{d}|^2 \omega^3 / 3\hbar c^3$  is the spontaneous decay rate of the levels  $|\pm\rangle$ ,  $|\vec{d}|$  is the magnitude of the dipole moment vector for the transitions  $|\pm\rangle \leftrightarrow |g\rangle$ ,  $N$  is the atomic number

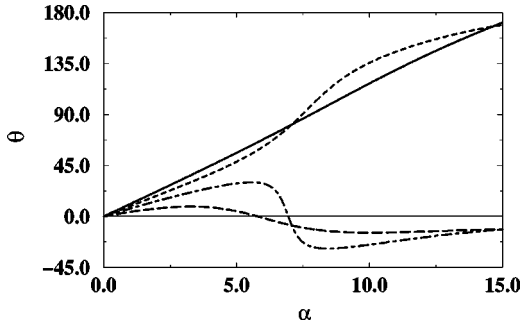


FIG. 2. Variation of MOR angle  $\theta$  (in degrees) with optical density  $\alpha$  for  $s=2\gamma$  and different laser linewidths  $\gamma_c=0.1\gamma$  (solid line),  $\gamma_c=0.5\gamma$  (dashed line),  $\gamma_c=\gamma$  (dot-dashed line), and  $\gamma_c=2\gamma$  (long-dashed line). We have chosen  $\lambda=422.67$  nm corresponding to  $^{40}\text{Ca } 1S_0 \leftrightarrow 1P_1$  transitions. Note the nonlinear dependence of  $\theta$  on  $\alpha$  for larger  $\gamma_c$ .

density, and  $s = \mu_B B / \hbar$  is the Zeeman splitting of the excited levels. Using these  $\chi_{\pm}$ , we can now write the field amplitude from Eq. (5) as

$$\vec{\mathcal{E}}_0 = [\hat{\epsilon}_+ \mathcal{E}_+ e^{i(\alpha/2)\rho_+} + \hat{\epsilon}_- \mathcal{E}_- e^{i(\alpha/2)\rho_-}], \quad (12)$$

where  $\alpha = 4\pi k l N |\vec{d}|^2 / \hbar$ ,  $\gamma = (3\lambda^2 / 2\pi) N l$  is the optical density of the medium.

In what follows, we will assume that  $\omega_l = \omega_{+g}(B=0)$ . We calculate the  $\langle I_n \rangle$ 's using Eqs. (10) and (9) numerically for different values of  $\gamma_c$  and  $s$ . We show the results in Fig. 2. We clearly see that for  $\gamma_c \ll s$  the rotation angle  $\theta$  is linearly proportional to  $\alpha$ . But for  $\gamma_c \gtrsim s$  this variation deviates from linearity in the large  $\alpha$  domain. This behavior can be explained in terms of the off-resonant components which dominate for large  $\gamma_c$  and large  $\alpha$ .

In order to understand the numerical results, we first consider the limit of small optical densities whence

$$S_1 = \frac{1}{2} [2 + \alpha \text{Re}\{i(\rho_+ + \rho_-)\}], \quad (13a)$$

$$S_2 = \frac{\alpha}{2} \text{Re}(\rho_- - \rho_+). \quad (13b)$$

Thus, the departure of the rotation angle from linearity has to do with the averages of the exponentials appearing in the  $I$ 's [Eq. (8)]. If one were to make the approximation of replacing all  $\chi$ 's in Eq. (8) by their averages, i.e.,

$$\langle \exp[2\pi i k l \chi_{\pm}] \rangle \equiv \exp[2\pi i k l \langle \chi_{\pm} \rangle], \quad (14)$$

then the Stokes parameters  $\langle S_1 \rangle$  and  $\langle S_2 \rangle$  would be

$$\langle S_1 \rangle = e^{-(\alpha/2)(\langle \rho_2^+ \rangle + \langle \rho_2^- \rangle)} \cos \left[ \frac{\alpha}{2} (\langle \rho_1^+ \rangle - \langle \rho_1^- \rangle) \right], \quad (15a)$$

$$\langle S_2 \rangle = -e^{-(\alpha/2)(\langle \rho_2^+ \rangle + \langle \rho_2^- \rangle)} \sin \left[ \frac{\alpha}{2} (\langle \rho_1^+ \rangle - \langle \rho_1^- \rangle) \right], \quad (15b)$$

where  $\langle \rho_{\pm} \rangle = \langle \rho_1^{\pm} \rangle + i \langle \rho_2^{\pm} \rangle$  and thus

$$\langle \theta \rangle = \frac{\alpha}{4} (\langle \rho_1^- \rangle - \langle \rho_1^+ \rangle) = \frac{1}{2} \frac{\alpha \gamma s}{(\gamma + \gamma_c)^2 + s^2}. \quad (16)$$

Clearly, the absorption does not contribute to the rotation angle. We have again recovered the linear dependence of  $\theta$  on  $\alpha$ , provided the approximation (14) is valid. Thus, any departure in linearity of  $\theta$  with respect to  $\alpha$  indicates the breakdown of the approximation (14). The numerical results of Fig. 2 clearly show the breakdown of the mean field description obtained by replacing the  $\chi$ 's by their average values.

From Eq. (16), we readily see that in the low  $\alpha$  domain, by increasing  $s$  (or  $\gamma_c$ ) while keeping  $\gamma_c$  (or  $s$ ) constant, the slope of  $\theta$  with  $\alpha$  decreases. This is clear from the numerical results of Fig. 2. Also, for larger values of  $\gamma_c$ , the variation of  $\theta$  with  $\alpha$  deviates from linearity. A linear variation of  $\theta$  with  $\alpha$  is attributed to a monochromatic laser field. If the electric field is spectrally impure, then the off-resonant components also contribute to  $\theta$ , through the relations (9), (6), and (7). Thus,  $\theta$  starts varying with  $\alpha$  linearly in the low  $\alpha$  limit, then saturates, and finally decreases to zero to change the direction of rotation for larger  $\gamma_c$  (see Fig. 2). But for smaller  $\gamma_c$  the linear behavior is retained even for larger  $\alpha$ , as the off-resonant components are not dominant in this parameter zone.

Next we consider the variation of the degree of polarization  $P$  and the ellipticity  $e$  with  $\alpha$ . We have noticed that  $P$  decreases from unity for increasing  $\alpha$ . This means that the output field no longer remains fully polarized; rather it becomes partially polarized.

Again, from Eqs. (6d), (8d), and (11), it is clear that an integration over the entire range of detuning  $\delta$  would yield  $\langle S_3 \rangle = 0$ , as the integrand is an odd function of  $\omega$ . Thus the ellipticity  $e$  becomes zero. This means that the polarized part of the output field remains linear.

From the above discussion, it is clear that the output field is rotated as a manifestation of cumulative effect of optical density, magnetic field, and laser linewidth. It also becomes partially polarized with no ellipticity.

#### IV. QUANTITATIVE MODELING OF EXPERIMENTAL RESULTS OF LABEYRIE *et al.* FOR MOR IN NONMONOCHROMATIC FIELDS

We now extend our understanding of resonant MOR as described in the previous section to explain the experimental data of Labeyrie *et al.* In their experiment, a cold atomic cloud of  $^{85}\text{Rb}$  is subjected to a static magnetic field. The laser probe beam passing through the medium in the direction of the magnetic field is tuned to the  $D_2$  line of the atoms ( $2S_{1/2} \leftrightarrow 2P_{3/2}$ ;  $\lambda = 780.2$  nm). Labeyrie *et al.* measured the intensities of outputs with different polarizations, as a function of laser detuning and also at different values of the optical density. They found a nonlinear dependence of the MOR angle  $\theta$  on optical density. They found that the linear behavior is recovered for larger magnetic field.

To explain these observations, we consider the relevant energy levels of  $^{85}\text{Rb}$  as used in the experiment (see Fig. 3).

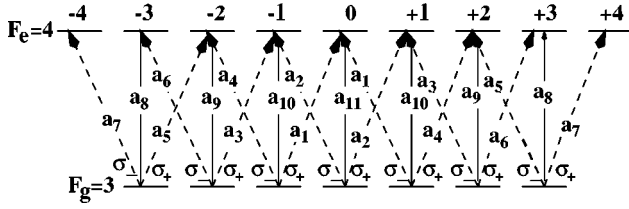


FIG. 3. Level diagram for the  $F_e=4 \leftrightarrow F_g=3$  transition. The numbers at the top of the figure indicate the magnetic quantum numbers of the sublevels. The relevant Clebsch-Gordan coefficients for the corresponding transitions are given by  $a_1 = -1/\sqrt{42}$ ,  $a_2 = -\sqrt{5}/3\sqrt{14}$ ,  $a_3 = -1/2\sqrt{21}$ ,  $a_4 = -\sqrt{5}/2\sqrt{21}$ ,  $a_5 = -1/6\sqrt{7}$ ,  $a_6 = -1/2\sqrt{3}$ ,  $a_7 = -1/3$ ,  $a_8 = -1/6$ ,  $a_9 = -1/\sqrt{21}$ ,  $a_{10} = -\sqrt{15}/6\sqrt{7}$ , and  $a_{11} = 2/3\sqrt{7}$ . The Zeeman splitting of the various sublevels is not shown.

The  $\hat{x}$ -polarized electric field (3) is applied to the cold  $^{85}\text{Rb}$  medium near resonantly. The medium is subjected to a uniform magnetic field  $\vec{B}$  applied in the  $z$  direction, i.e., along the direction of propagation of Eq. (3).

#### A. Calculation of $\chi_{\pm}$ and optical density

The circular components  $\sigma_{\pm}$  of the input electric field (3) interact with the transitions  $m_e \leftrightarrow m_g = m_e - 1$  and  $m_e \leftrightarrow m_g = m_e + 1$ , respectively. We assume that the electric field is weak enough so that it is sufficient to use the linear response of the system to the laser field. We neglect the ground-state coherences. As we are considering cold atoms, we neglect the collisional relaxations and Doppler broadening of the sublevels. We also assume that the atomic population is equally distributed over all the ground sublevels.

Using all these assumptions, we can write the susceptibilities  $\chi_{\pm}$  for the  $\sigma_{\pm}$  components as the sum of the susceptibilities of all the relevant  $m_e \leftrightarrow m_g$  transitions in the following way:

$$\chi_{\pm} \equiv \sum_{m_e, m_g} \frac{1}{7} \frac{N |\vec{d}_{m_e, m_g} \cdot \hat{\epsilon}_{\pm}|^2}{\hbar} \frac{i}{\Gamma_{m_e, m_g} + i(\delta + s_{m_e, m_g})}, \quad (17)$$

where  $s_{m_e, m_g} = (g_g m_g - g_e m_e) s$  is the relative amount of the Zeeman shift of the excited sublevel  $m_e$  with respect to the

Zeeman shifted ground sublevel  $m_g$ , and  $g_g = 1/3$  and  $g_e = 1/2$  are the Landé  $g$  factors of the ground and excited levels, respectively. The factor  $1/7$  comes into the expression (17) as we have assumed equal population distribution in all the  $(2F_g + 1) = 7$  ground sublevels. The coherence relaxation rate  $\Gamma_{m_e, m_g}$  in Eq. (17) is given by

$$\Gamma_{m_e, m_g} = \frac{1}{2} \sum_k \gamma_{k, m_e}, \quad (18)$$

where  $\gamma_{i, j}$  is the spontaneous relaxation rate from the sublevel  $j$  to  $i$ . Here we have assumed that there is no spontaneous relaxation from the ground sublevels. The terms  $\vec{d}_{m_e, m_g}$  and  $\Gamma_{m_e, m_g}$  can be calculated from the relevant Clebsch-Gordan coefficients (see Fig. 3) [6]. The Einstein  $A$  coefficient for the  $D_2$  line is known to be

$$A = \frac{4\omega^3}{3\hbar c^3} \frac{|(J = \frac{3}{2} \|D\| J' = \frac{1}{2})|^2}{4} = \frac{4\omega^3}{3\hbar c^3} \frac{|(\frac{3}{2}, \frac{5}{2}, 4 \|D\| \frac{1}{2}, \frac{5}{2}, 3)|^2}{9}, \quad (19)$$

where  $(\|D\|)$  represents the reduced matrix element of the dipole moment vector  $\vec{d}_{m_e, m_g}$ . The three symbols  $3/2$ ,  $5/2$ , and  $4$  correspond to the  $J$ ,  $I$ , and  $F$  values, respectively, of the upper levels. Thus all  $\Gamma_{m_e, m_g}$ 's in Eq. (17) are found to be equal to  $(4\omega^3/3\hbar c^3) |(\frac{3}{2}, \frac{5}{2}, 4 \|D\| \frac{1}{2}, \frac{5}{2}, 3)|^2/2$ .

We calculate the optical density  $\alpha$  of the medium, when the input light field is resonant with the  $m_e = 0 \leftrightarrow m_g = 0$  transition ( $\delta = 0$ ) in the absence of any magnetic field ( $B = 0$ ). For this, we first obtain the total output intensity from Eq. (6a) averaged over a very narrow laser line shape, i.e., in the limit  $\gamma_c \rightarrow 0$ . Using Eq. (17), we thus find that the transmittivity of the medium becomes

$$T = \frac{1}{I_0} \langle S_0 \rangle_{\gamma_c \rightarrow 0} = \frac{1}{I_0} S_0|_{\delta=0} = \exp(-\alpha), \quad (20)$$

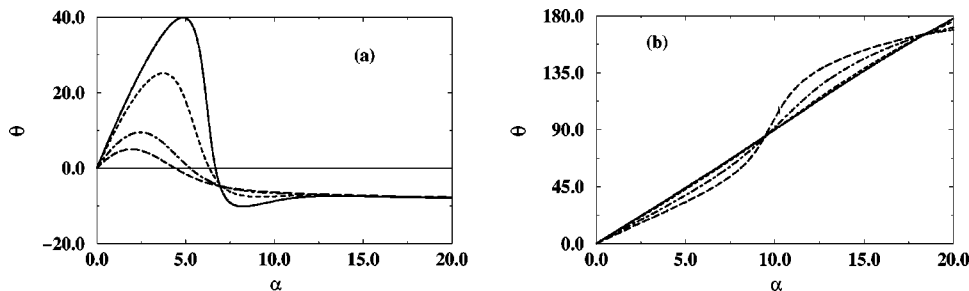


FIG. 4. Variation of magneto-optical rotation angle  $\theta$  (in degrees) with  $\alpha$  for magnetic field (a) 2 G ( $\equiv 2\pi \times 2.8$  MHz) and (b) 8 G ( $\equiv 2\pi \times 11.2$  MHz) for laser linewidths  $2\gamma_c = 2\pi \times 0.5$  MHz (solid line),  $2\gamma_c = 2\pi \times 1$  MHz (dashed line),  $2\gamma_c = 2\pi \times 3$  MHz (dot-dashed line), and  $2\gamma_c = 2\pi \times 5$  MHz (long-dashed line). The dot-dashed curves correspond to the width of the laser used in the experiment [4]. Note that the linewidth of the  $D_2$  line is  $2\pi \times 5.88$  MHz.

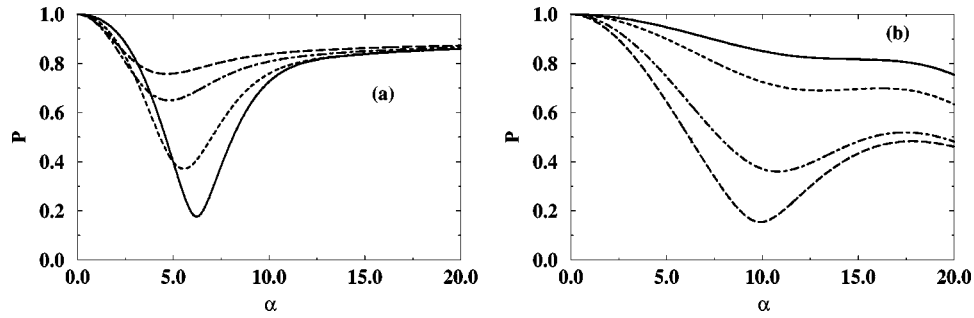


FIG. 5. Variation of degree of polarization  $P$  with  $\alpha$  is shown for magnetic field (a) 2 G and (b) 8 G, for laser linewidths  $2\gamma_c = 2\pi \times 0.5$  MHz (solid line),  $2\gamma_c = 2\pi \times 1$  MHz (dashed line),  $2\gamma_c = 2\pi \times 3$  MHz (dot-dashed line), and  $2\gamma_c = 2\pi \times 5$  MHz (long-dashed line). The dot-dashed curves correspond to the width of the laser used in the experiment [4].

where  $\alpha = (3/7)(3\lambda^2/2\pi)NI$ . It should be borne in mind that it is different from the definition in Sec. III.

### B. Discussions

Using the above expressions for  $\chi_{\pm}$  [Eq. (17)] and Eq. (9), we calculate the averaged intensities  $\langle I_i \rangle$  in different polarization directions. The Stokes parameters  $S_{\alpha}$ , degree of polarization  $P$ , and Faraday rotation  $\theta$  are calculated using the relations (7). In Fig. 4, we show how the Faraday angle  $\theta$  varies with the optical density  $\alpha$  for different values of  $\gamma_c$  and  $B$ . Clearly, for  $\gamma_c \ll s$ , the rotation angle  $\theta$  varies linearly with  $\alpha$ . But for larger  $\gamma_c$  ( $\geq s$ ) the variation of  $\theta$  with  $\alpha$  deviates from linearity in large  $\alpha$ . This is because the off-resonant components contribute to the output intensity. Also, note that for a given value of  $\gamma_c$ , if  $s$  is increased, the linearity is maintained even in the large  $\alpha$  domain. This is because for larger  $s$ , the off-resonant components do not contribute much to the output intensity. The resonant frequency component is always dominant in the optical density range

considered. We also note that, as  $\gamma_c$  increases, the linear slope of  $\theta$  with  $\alpha$  decreases in the small  $\alpha$  domain.

In Fig. 5, we show the variation of the degree of polarization  $P$  with  $\alpha$  for various values of  $B$  and  $\gamma_c$ . These results reveal that, with increase in  $\alpha$ , the degree of polarization deviates from unity, i.e., the output electric field not only rotates in polarization, but also becomes *partially* polarized. However, the ellipticity of the output field still remains zero as we argued in Sec. III.

### V. CONCLUSIONS

In summary, we have given a quantitative analysis of the magneto-optical rotation of spectrally impure fields in optically thick cold  $^{85}\text{Rb}$  atomic medium. We have shown that the dependence of rotation on the optical density of the medium deviates from linearity due to the finite laser linewidth. Using our model, we explained the experimental results of Labeyrie *et al.*

- 
- [1] D. Budker, W. Gawlik, D. F. Kimball, S. M. Rochester, V. V. Yashchuk, and A. Weis, *Rev. Mod. Phys.* **74**, 1153 (2002).  
 [2] J.-P. Connerade, *J. Phys. B* **16**, 399 (1983).  
 [3] G. S. Agarwal, P. Anantha Lakshmi, J.-P. Connerade, and S. West, *J. Phys. B* **30**, 5971 (1997).  
 [4] G. Labeyrie, C. Miniatura, and R. Kaiser, *Phys. Rev. A* **64**,

033402 (2001).

- [5] M. Born and E. Wolf, *Principles of Optics*, 7th ed. (Cambridge University Press, Cambridge, 1999), p. 630.  
 [6] I. I. Sobel'man, *Atomic Spectra and Radiative Transitions*, 2nd ed. (Springer-Verlag, Berlin, 1992), Sec. 9.3.6.